HHS Public Access

Author manuscript

Exp Cell Res. Author manuscript; available in PMC 2024 December 15.

Published in final edited form as:

Exp Cell Res. 2023 December 15; 433(2): 113852. doi:10.1016/j.yexcr.2023.113852.

ADAMTS-1 has nuclear localization in cells with epithelial origin and leads to decreased cell migration

Suély V. Silva[a,1], **Maíra A. Lima**[a,b,1], **Louis Hodgson**[b], **Juan Carlos Rodríguez-Manzaneque**[c], **Vanessa M. Freitas**[a,*]

[a]Department of Cell and Developmental Biology, Biomedical Sciences Institute, University of São Paulo, São Paulo, Brazil

[b]Department of Molecular Pharmacology, Albert Einstein College of Medicine, Bronx, NY, USA

[c]GENYO, the Center for Genomics and Oncological Research, Avenida de la Ilustración, 114, Granada 18016, Spain

Abstract

In the study of tumorigenesis, the involvement of molecules within the extracellular matrix (ECM) is crucial. ADAMTSs (A Disintegrin and Metalloproteinase with Thrombospondin motifs), a group of secreted proteases known for their role in ECM remodeling, were primarily considered to be extracellular proteases. However, our research specifically detected ADAMTS-1, a member of this family, predominantly within the nucleus of mammary cells. Our main objective was to understand the mechanism of ADAMTS-1 translocation to the nucleus and its functional significance in this cellular compartment. Our investigation uncovered that nuclear ADAMTS-1 was present in cells exhibiting an epithelial phenotype, while cells of mesenchymal origin contained the protease in the cytoplasm. Moreover, disruption of ADAMTS-1 secretion, induced by Monensin treatment, resulted in its accumulation in the cytoplasm. Notably, our research indicated that alterations in the secretory pathways could influence the protease's compartmentalization. Additionally, experiments with conditioned medium from cells containing

*Corresponding author: vfreitas@usp.br (VMF), Department of Cell and Developmental Biology, Biomedical Sciences Institute, University of Sao Paulo, Av. Prof. Lineu Prestes, 1524 Room 428, Zipcode: 05508-000, Sao Paulo- Brazil.

[1]These authors contributed equally to this work

CRediT Authorization Contribution Statement

Suély V. Silva: Writing – original draft, Visualization, Validation, Resources, Methodology, Investigation, Funding acquisition, Formal analysis, Data curation, Conceptualization. **Maíra A. Lima:** Writing – review & editing, Writing – original draft, Methodology, Investigation, Formal analysis. **Louis Hodgson:** Writing – review & editing, Writing – original draft, Resources, Funding acquisition. **Juan Carlos Rodríguez-Manzaneque:** Resources, Funding acquisition. **Vanessa M. Freitas:** Writing – original draft, Supervision, Resources, Project administration, Methodology, Funding acquisition, Data curation, Conceptualization.

Declaration of competing interest:

The authors declare that they have no known competing financial interests or personal relationships that could have appeared to influence the work reported in this paper.

Ethics approval and consent to participate:

This study was exempted by ICB/USP Ethics Committee on Research (Protocol/CEP-ICB no. 708/15)

During the preparation of this work the author(s) used ChatGPT in order to improve the fluidity of the text. After using this tool/ service, the author(s) reviewed and edited the content as needed and take(s) full responsibility for the content of the publication.

nuclear ADAMTS-1 demonstrated its internalization into the nucleus by HT-1080 cells and fibroblasts. Furthermore, heightened levels of ADAMTS-1 within the ECM reduced the migratory potential of mesenchymal cells. This highlights the potential significance of nuclear ADAMTS-1 as a critical component within the tumor microenvironment due to its functional activity in this specific cellular compartment.

Keywords

Breast cancer; Extracellular matrix; Proteolysis; Nucleus; Endocytosis; ADAMTS-1

1. Introduction

The ADAMTS proteinases belong to a family of 19 metalloproteinases (1, 2) that participate in extracellular matrix processing (3), organogenesis (4), and hemostasis (5). They have also been identified to be expressed during ovulation (6). While they are not membrane-anchored proteinases, they do attach to the extracellular matrix after being secreted (1, 7–10). One distinguished member of this family is ADAMTS-1, a well-known extracellular matrix protease (1, 2, 9, 10) and the first described member of the ADAMTS family of metalloproteases (11, 12). This secreted protease consists of six domains, namely, 1) a pro-domain, 2) a metalloproteinase, 3) a disintegrin-like domain, 4) a thrombospondin (TSP) homologous domain containing TSP type I motif, 5) a spacer region, and 6) C-terminus TSP submotifs (13). The maturation of ADAMTS-1 requires two independent and sequential processing events that may release two forms of the protein. With the cleavage of the prodomain from the 110 kDa zymogen, an 87 kDa active form remains which can be further processed by removal of the catalytic subunit from the TSP repeats, leaving the C-termianl 65 kDa soluble form. The proteolytic deletion of the last two TSP repeats is probably significant for the in vivo function of this protein (14). Apart from its role in the extracellular matrix, our prior research has demonstrated that 87 kDa ADAMTS-1 is present within the nuclei of the three cell lines studied and plays a proteolytic role on the aggrecan substrate. Additionally, similar proteases such as ADAMTS-4 and ADAMTS-5 were found in the cytoplasm and extracellular compartment, emphasizing that nuclear localization is specific to the aggrecanase ADAMTS-1 (15).

The function of nuclear ADAMTS-1 remains unclear. However, our previous publication demonstrated the proteolytic activity of ADAMTS-1 within the nucleus by cleaving aggrecan, one of its substrates that was also present in the nucleus (15). Additionally, other ADAMTS-1 substrates, like versican, have been identified in the nucleus, where they appear to play a role in organizing the mitotic spindle during cell division (16). Other proteases and protease inhibitors have also been identified in the nucleus, such as MMP-2 and -3 and the metalloprotease inhibitor TIMP-1 (17–20). MMP-3 fragments were reported in the nucleus of tumor cell lines, including HepG2 cells and liver myofibroblasts and is involved in apoptosis (17). A study conducted by Kwan and colleagues indicated the presence of MMP-2 in the nucleus of cardiac myocytes, where it cleaves poly (ADP-ribose) polymerase (PARP) in vitro (20), enzymes that play a vital role in various cellular processes, including the modulation of chromatin structure, transcription, replication, recombination,

and DNA repair (21). Our research group demonstrated in this study that the localization of ADAMTS-1 in mesenchymal cells differs from that in epithelial cells. Specifically, epithelial cells exhibit ADAMTS-1 in both the nuclear and extracellular compartments, whereas in mesenchymal-derived cells, it is present in the cytoplasmic and extracellular compartments.

Moreover, fibroblasts exposed to conditioned media from epithelial cells also exhibit ADAMTS-1 in their nuclei, likely due to endocytosis. Additionally, the nuclear localization could be altered when the Golgi Apparatus function and architecture are disrupted. When ADAMTS-1 secretion is impaired, it becomes dispersed throughout the cytoplasm, but not in the cell nuclei. This indicates that secretion is crucial for nuclear localization, presumably because the protease needs to be secreted and subsequently endocytosed to reach the nuclei. Considering that ADAMTS-1 is a well-known metalloproteinase found in the extracellular matrix, where it interacts with its substrates, causing remodeling (2, 22), it is imperative to identify the ADAMTS-1 interaction partners in the nuclei. Hence, the objective of this project was to investigate how ADAMTS-1 translocates to the cell nuclei and identify its interaction partners.

2. Materials and methods

2.1. Cell culture

MDA-MB-231, MCF-7, MDAH-2774, HTR-8, NIH OVCAR-3, fibroblasts (Nontransformed mammary fibroblasts were expanded from primary cultures derived from normal human breast tissue obtained from esthetic mammoplasty of a 22 year-old patient (23)), parental HEK-293T cells and a well-established lineage of cells that overexpress ADAMTS-1, called HEK-293T MPA (mcherry puromycin ADAMTS-1) and your control cell line HEK-293T MPC (mcherry puromycin Control) and HT1080 wild type, HT1080 ADAMTS-1 full length (ATS1) or ADAMTS-1 with a mutation in the catalytic domain (Z11), which the mutation consisted in the single substitution of residue E385 to A at the zinc-binding site to disable the catalytic activity of ADAMTS1 (Acquired through collaboration with Professor Juan Carlos Rodríguez-Manzaneque's laboratory (24)), were cultivated in Dulbecco's modified Eagle's medium/Diluted with nutrient F-12 at the 1:1 ratio (DMEM/F-12, Sigma Chemical Co, St Louis, MO, USA), supplemented with 10% fetal bovine serum (FBS Cultilab, Campinas, Brazil). The MCF-10A cell line, obtained from normal mammary epithelium, was cultivated in DMEM/F-12, with the addition of 5% horse serum, 20 ng/ml EGF, 0.5 mg/ml hydrocortisone, 10 mg/ml insulin, and 100 ng/ml cholera toxin. The MUM-2B cells were cultured in Roswell Park Memorial Institute-1640 medium (RPMI-1640, HyClone, Thermo Scientific, USA), supplemented with 10% fetal bovine serum (FBS Cultilab, Campinas, Brazil), 100 IU/mL of penicillin G sodium, and 100 mg/mL of streptomycin sulfate. Cells were maintained in 75 cm2 flasks at 37 °C in an atmosphere containing 5% CO2. Cell growth was monitored daily under an inverted phase contrast microscope. Representative samples of the culture were later frozen and kept in liquid nitrogen, cryoprotected with 10% dimethyl sulfoxide (DMSO, Sigma).

2.2. Treatment of cell lines with conditioned medium from HT1080 or HEK293T cells overexpressing ADAMTS-1

HEK293T cells overexpressing ADAMTS-1 were established as described previously and termed HEK293T-MPA-mcherry/puromycin/ADAMTS-1 (25). Shaw et al. (26) performed a HEK293 microarray analysis and no transcript of any member of ADAMTS's family was detected. The increase in ADAMTS-1 levels in the transduced cells was verified by Western blotting. HEK293T cells or MDA-MB-231 were plated on 100 mm cell culture plates and when reached 90% of confluence, 10 mL of DMEM/Ham's F-12 medium without SFB was added and conditioned for 24 h, the collected medium was centrifuged and filtered in a syringe with 0.45 membrane filter to remove cell debris. The obtained medium was pooled, aliquoted and then frozen at − 80 °C. The same conditioned medium was used in the experiments that were carried out. The cell lines were treated with either the ADAMTS1 enriched media (MPA) or the conditioned medium from the control HEK293T cells without ADAMTS-1 overexpression (MPC).

2.3. Immunofluorescence

2 × 10^5 cells were grown on glass coverslips for 24 hours. Subsequently, they were fixed in 4% paraformaldehyde in 1X phosphate-buffered saline (PBS) for 10 minutes, rinsed, and permeabilized with 0.5% Triton X-100 (Sigma) in PBS for 10 minutes. After another round of rinsing, the cells were blocked with 10% normal goat serum (KPL, Gaithersburg, USA) for 1 hour. The cells were then incubated with primary antibodies against ADAMTS-1 at a dilution of 1:1000 in 0.1% BSA (ab28284, Abcam- Aminoterminal end), Golgin 97 (12640-1-AP Thermo Fisher) at a dilution of 1:50 in 0.1% BSA, and NFkB p65 (14-6731-81 Thermo Fisher) at a dilution of 1:100 in 0.1% BSA overnight. All the antibodies used were rabbit polyclonal, and the incubation was conducted for 1 hour at room temperature. Following this, the coverslips were washed three times for 5 minutes with PBS and incubated with a secondary antibody conjugated to the fluorophore Goat anti-Rabbit IgG Alexa Fluor 568 (# A-11011 Invitrogen, Eugene, Oregon, USA) at a concentration of 1:200, diluted in 10% Normal Goat Serum (KPL, Gaithersburg, USA) for 1 hour in the dark. Subsequently, the coverslips were washed with PBS and incubated with Phalloidin-Alexa 488 (#A12379 - Life Technologies, Carlsbad, CA, USA) at a concentration of 1:100, diluted in PBS for 15 minutes in the dark. Finally, the coverslips were mounted with Prolong Gold antifade reagent with DAPI (#P36941- Invitrogen, Eugene, Oregon, USA). An irrelevant rabbit IgG antibody was used as the negative control.

2.4. Western Blotting

We analyzed three components: the conditioned medium (representing the secreted material), the nuclear fraction, and the cytosolic fraction. To precipitate the conditioned medium, we collected the medium in tubes containing a protease inhibitor. The sample was then precipitated and resuspended in the lysis buffer (50 mM sodium acetate, 150 mM sodium chloride, 10% glycerol (v/v), and degassed ddH2O). Cell fractions were obtained using the NEPER Reagent for nuclear and cytoplasmic protein extraction kit in accordance with the manufacturer's instructions (Pierce, Rockford, IL). Electrophoresis was conducted following the SDS-PAGE method. We loaded 30 μg of protein per well, which were then

separated on a 10% polyacrylamide gel. After electrophoresis, the proteins were transferred to nitrocellulose membranes (Amersham, GE Healthcare Life Science, Pittsburgh, USA), and these membranes were blocked with 5% milk in TBS-tween (TTBS) before incubation with antibodies that recognize the ADAMTS-1 protein (1:1000 MAB1810 -Millipore Corporation -Myc-His carboxyl tagged full-length recombinant protein based on the human sequence). This primary antibody was detected using a peroxidase-conjugated secondary antibody (ab6728-Abcam 1:2000). To enable labeling with more than one antibody, the membranes were stripped using the “Restore Western Blot Stripping Buffer” (Pierce) and subjected to new labeling. As a loading control, we used the primary antibody anti-histone histone (1:4000 in 0.1% BSA, Millipore 05–457) for the nuclear fraction and GAPDH (1:1000 in 0.1% BSA, 14C10-Rabbit mAb #2118, Cell Signaling) and β-actin (1:1000 in 0.1% BSA, Abcam-ab8227) for the cytoplasmic fraction.

2.5. Analysis of the ADAMTS-1 and chromatin interaction

For the immunofluorescence experiment, fixed cells were prepared using 4% paraformaldehyde in 1X PBS. Subsequently, cells underwent treatment with Buffer A (10 mM PIPES pH 6.8; 100 mM NaCl; 300 mM sucrose; 3 mM MgCl2; 1 mM EGTA; 0.5% Triton X-100; 1 mM PMSF) at 4°C for 10 minutes, effectively removing the plasma membrane, soluble proteins in the cytoplasm, and nucleoplasm. Core proteins were then extracted with a brief exposure to Buffer B (10 mM PIPES pH 6.8; 250 mM (NH4)2SO4; 300 mM sucrose; 3 mM MgCl2; 1 mM EGTA; 0.5% Triton X-100; 1 mM PMSF) at 4°C for 5 minutes. Subsequent digestion of the remaining chromatin was performed with DNase I (deoxyribonuclease I) in a digestion buffer-Buffer C (10 mM PIPES pH 6.8; 50 mM NaCl; 300 mM sucrose; 3 mM MgCl2; 1 mM EGTA; 0.5% Triton X-100; 1 mM PMSF) at 4°C for 1 hour, followed by washing with buffer B. The structures remaining after individual treatment with each buffer were then fixed with 3% paraformaldehyde in PBS at 25°C for 15 minutes, and subsequently incubated for 1 hour with the primary histone H1 antibody (Sigma, H1917) at 1:100 in 0,1 BSA. Specific binding was detected using the Alexa Fluorine fluorophore-conjugated secondary antibody (Invitrogen, Eugene, Oregon, USA). The observations were made using a conventional fluorescence microscope.

2.6. Analysis of ADAMTS-1 Endocytosis

We utilized Dynasore (Sigma, D7693) at a concentration of 80 μM. Dynasore is a drug that functions by inhibiting the action of the protein dynamin, which plays a crucial role in the fusion of endocytic vesicles (27). For these assays, we employed cells with a density ranging from 40% to 70%. Cultures that are more confluent tend to be more resistant to the effects of the drug. To assess the results of incubating cells with Dynasore, we conducted immunofluorescence. 24 hours after plate, the cells were washed thrice with culture medium devoid of fetal bovine serum (FBS) and kept in culture for 2 hours to induce nutrient starvation. Following this period, the cells were treated with 80 μM Dynasore for 24 hours. The control sample was maintained in culture medium without the addition of supplements, containing 0.2% DMSO (Sigma) as the vehicle.

2.7. Endocytosis analysis

HT-1080 was selected for this assay because it does not display the nuclear localization pattern of ADAMTS-1, making it suitable model for monitoring the potential endocytosis of the protease. Cells plated on coverslips were subjected to 1-hour or 24-hour starvation. Subsequently, conditioned medium from MDA-MB-231, HEK-293T MPC, and HEK293T MPA cells was added to these cells for 1 hour or 24 hours in the presence or absence of Dynasore. The treatment involved the use of 80 μM Dynasore (Sigma Aldrich) added to the culture medium. Samples from the control group were maintained in culture medium containing DMSO, which served as Dynasore's dilution vehicle, with the volume equivalent to that added to cells treated with Dynasore. As a positive control for the assay, we employed the Anti-β-integrin antibody (I8638 Sigma-Aldrich) at a 1:100 dilution in 0.1% BSA conjugated with Alexa-568 fluorophore (Invitrogen, Eugene, Oregon, USA) for the HT-1080 cells. The antibody was incubated with the live cells for 2 hours at 37°C, and the endocytosis of this molecule was monitored in the presence of Dynasore or the vehicle (DMSO, Sigma).

2.8. Blocking ADAMTS-1 exocytosis

To inhibit the exocytosis of ADAMTS-1, we employed Monensin (ab 120499) in our assay. This compound effectively blocked protein export by the Golgi apparatus. Subsequently, we conducted cell fractionation, followed by analysis using Western Blot and immunofluorescence techniques. For the immunofluorescence assay, cells were seeded on coverslips in a culture medium suitable for the specific lineage at a concentration of 2×10^5 cells for 24 hours. Meanwhile, for the Western blotting procedure, cells were plated in 100 mm × 20 mm plates with a suitable growth medium for each cell line at a concentration of 1×10^6 cells for 24 hours. Before treatment, the cells were washed thrice with culture medium devoid of serum, and then maintained in culture for 2 hours to induce nutrient starvation. Following the starvation period, the cells were exposed to 2 μM Monensin for 24 hours in a complete medium supplemented with 10% fetal bovine serum.

2.9. Analysis of ADAMTS-1 Secretion

To verify whether the secretion of ADAMTS-1 contributes to the nuclear localization of the protease, we assessed the secretory profile of the protease using Heparin. Heparin prevents protease cleavage from occurring, leading to its secretion in its complete form. We seeded cells for immunofluorescence and western blotting as per the described protocol, for duration of 24 hours. Subsequently, the cells underwent three washes with culture medium lacking FBS and were maintained in culture for an additional 2 hours to induce nutrient starvation. Following this period, the cells were exposed to 5 μg/ml heparin, diluted in culture medium without FBS, for 24 hours. Post-treatment, the cells were fixed to Immunofluorescence analysis or they were lysed, and the culture medium was collected for analysis of the conditioned medium by Western Blot.

2.10. Blockade of nuclear pore-mediated transport using Importazole

To investigate whether ADAMTS-1, initially present in the cytoplasm of mesenchymal cells, could be transported to the nucleus through the cytoplasmic-nuclear transport, we employed

Importazole. Cells were plated for immunofluorescence and western blotting, following the specified protocol, over a 24-hour period. Subsequently, the cells underwent three washes with culture medium devoid of FBS and were then subjected to a 2-hour period of nutrient starvation. Following this, the cells were treated with 50 μM of Importazole (Sigma Aldrich) diluted in DMSO for 5 hours in serum-free medium, followed by treatment with 10 ug/ml of LPS (Sigma Aldrich) for 1 hour. Post-treatment, cells were washed with 1X PBS, and serum-free medium was introduced for a 24-hour period to evaluate the conditioned medium and cell lysate. Control cells were cultured in medium containing DMSO (Sigma) (the Importazole dilution vehicle) in a volume equivalent to that added to the Importazole-treated cells.

2.11. Wound healing assay

The cells were cultivated in 35 mm diameter plates until they achieved 80% confluence. Subsequently, a “wound” was generated in the monolayer by gently passing a 10 μL pipette tip over it. This action led to a disruption in the monolayer, causing the cells at its edges to migrate towards the vacant spaces. Reference points were designated at the base of each plate to facilitate capturing photomicrographs of the same regions of the “wounds” at different intervals (0 and 24 hours). Cell migration was assessed by measuring the unoccupied area (marked arbitrarily as a region lacking cells) using the Image J program, a public domain software developed by Wayne Rasband, NIMH, NIH, USA. The cell migration index was determined by the percentage decrease in the “wound” area.

2.12. Viability by Trypan Blue dye exclusion analysis

Trypan blue (Sigma Chemical Co., St. Louis, MO, USA) was used to determine the number of viable cells present in the cell suspension. Each 10 μl of the cell suspension was mixed to 10 μl Trypan blue. Then the cells were examined by the Countess™ II Automated Cell Counter equipment (Thermo Fischer, Waltham, Massachusetts, USA) to determine if the cells absorbed or deleted the dye. Cells that absorbed the dye were defined as non-viable; those that excluded were considered viable.

2.13. Transwell migration assay

Polycarbonate membranes with 8 μm pores in 10-well Boyden chambers (Neuro Probe ®) were used for the migration assays. In migration assays, 1×10^5 cells were plated into the upper chamber containing 800 μL of DMEM/F12 medium with 1% serum. The lower chamber was filled with 800 μL of DMEM/F12 with 5% serum and incubated under standard cell culture conditions for 24 h. Following the incubation, the membrane with the cells was fixed with 4% paraformaldehyde and postfixed with 0.2% crystal violet in 20% methanol. Cells on the upper side of the filter were removed with a cotton swab. The migrated cells on the lower side of the filter were photographed and counted.

2.14. Statistical analyzes

The data is presented as the mean and standard deviation. Analysis of the variance between groups was conducted using analysis of variance (ANOVA), followed by post-hoc

Bonferroni multiple comparisons, performed with GraphPad Prism 5 software (GraphPad, San Diego, CA). Statistically significant differences were considered for $p \leq 0.05$.

3. Results

3.1. Localization of ADAMTS-1 in different cell types

When assessing the localization of ADAMTS-1 in various cell types with mesenchymal/epithelial origins and phenotypes, we noted that the distribution of ADAMTS-1 varies depending on the cell's origin (Table1). As depicted in Fig 1A, a distinct nuclear/nucleolar localization of ADAMTS-1 is evident in HTR-8, MDAH-2774, NIH-OVCAR-3 and MDAH-MB-231. Conversely, in Fibroblasts, Mum-2B and HT-1080, ADAMTS-1 is dispersed throughout the cytoplasm, devoid of nuclear/nucleolar labeling (Fig 1B, C). We used the HT1080 cell line expressing ADAMTS-1, with a mutation involving the single substitution of residue E385 with A in the zinc binding site to deactivate the catalytic activity of ADAMTS1. This was done to investigate whether mutations in the catalytic domain could result in the translocation of ADAMTS-1 into the nucleus. The findings revealed that ADAMTS-1 with the mutation (Z11), along with its controls ATS1 and wild type, remained in the cytoplasm of HT1080 cells (Fig 3 C). Our observations indicate that the presence of ADAMTS-1 in the nucleus is not uniform across all cell types. Specifically, nuclear ADAMTS-1 is observed in cells of epithelial origin, whereas in cells of mesenchymal origin, the protease predominantly localizes to the cytoplasm. Similar findings, indicating the presence of ADAMTS-1 in the nucleus, were also noted in the MCF-10A and MCF-7 cell lines (Supplementary figures 1 and 2, respectively). The analyses were conducted in technical and biological triplicates, and Figure 1 displays representative images of the findings.

3.2. ADAMTS-1 is strongly associated with nuclear structures.

To explore whether ADAMTS-1 associates with any specific structure within the nucleus, we conducted subcellular fractionation experiments on coverslips. Initially, cells cultured on coverslips were treated with a buffer containing 0.5% Triton X100 (referred to as Buffer A). This treatment effectively eliminated the plasma membrane, soluble proteins in the cytoplasm, and the nucleoplasm. At this stage, partial removal of actin filaments (β-actin) was observed, as indicated in Fig 2 (Buffer A) by the reduction in the intensity of actin filament labeling and the consequent decline in the cytoskeleton's microtubules in these cells. This trend persisted as additional buffers were introduced. Subsequent exposure to a high-salt solution (referred to as Buffer B) led to an approximately 50% reduction in histone H1 in the MDA-MB-231 cell line (Fig 2 – Buffer B). Further treatment with the Buffer C + Dnase I nearly eradicated the histone signal, also demonstrated in Fig 2 (Buffer C). Notably, despite these successive washes, the protease persisted within the nucleus of the cells, suggesting that ADAMTS-1 tightly associates with specific nuclear structures, excluding DNA. Analyses were performed in triplicates, both technically and biologically, with Figure 2 presenting illustrative images of the results.

3.3. The importation of nuclear ADAMTS-1 is not carried out by importins, but the Golgi apparatus is involved in the compartmentalization of the nuclear protease.

To investigate the nuclear internalization mechanism of ADAMTS-1, we initiated a series of experiments targeting endocytosis and secretion. By pre-treating the cells with Monensin, which disrupts the Golgi apparatus and consequently affects the secretion of molecules to the ECM, we determined the protease's localization. In Fig 3A, we observed that incubating MDA-MB-231 cells with 2 μM of Monensin induced a shift in ADAMTS-1 compartmentalization. Notably, a diffuse distribution of ADAMTS-1 throughout the cell cytoplasm was evident, with no indication of nuclear compartmentalization. This stark disparity is clear when comparing the treated cells with the control group (Fig 3A).
To confirm Monensin's efficacy, we conducted additional immunofluorescence targeting a protein responsible for maintaining the Golgi apparatus structure. Post-treatment, cell dilation was observed, and examination of Golgina 97 immunolocalization demonstrated significant dispersion within the cell cytoplasm, in contrast to its typical perinuclear location in the control sample (Fig 3B). Similar observations were noted regarding ADAMTS-1 protein expression. A comparison between the control and Monensin-treated cells revealed heightened protein expression in the cytoplasm, with no observable protease expression in the nuclear compartment (Fig 3C). Furthermore, regarding the conditioned medium, we observed a failure of the treated cells to secrete the protease into the extracellular medium. To assess whether the protease could be transported to the nucleus using the importin-mediated active transport pathway, we conducted experiments treating cells with Importazole (IPZ). Importazole is an inhibitor of the transport receptor importin-β (Karyopherin beta), specifically obstructing importin-β-mediated nuclear import while leaving transportin-mediated nuclear import or CRM1-mediated nuclear export intact. Upon administering 100 μM IPZ, we noted that the protease's localization remained nuclear in comparison to the control (Fig 3D). This observation suggests that ADAMTS-1 does not rely on importin-β for nuclear entry.

As a control and to assess the efficacy of the import blockade caused by Importazole (IPZ), the cells underwent treatment with lipopolysaccharide (LPS). LPS is known to stimulate the nuclear localization of the transcription factor NFκB p65. In Fig 3E, we observed that LPS treatment triggered p65 NFκB translocation to the nucleus, whereas cells treated with Importazole exhibited reduced p65 NFκB within the nucleus.

All the analysis was conducted three times each, both technically and biologically, and Figure 3 illustrates the findings.

3.4. Heparin alters the ADAMTS-1 secretion profile, but not the amount of nuclear ADAMTS-1

Our subsequent approach involved using Heparin to investigate whether the treatment could alter the nuclear localization of ADAMTS-1. While assessing changes in the levels of ADAMTS-1 protein expression, we noticed that the treatment of MDA-MB-231 cells with Heparin led to a statistically significant increase in the expression of proteins secreted into the ECM (Fig 4 A, B). However, in both the cytoplasmic and nuclear compartments, the treatment did not induce any changes in the protein levels of the protease, nor were there

any alterations in the localization of ADAMTS-1 (Fig 4 C, D). During the evaluation of the effects of Heparin treatment through immunofluorescence, we observed that there was no statistically significant difference concerning the amount of ADAMTS-1 in the nucleus or nucleolus (Fig. 4G). However, there was a notable difference in the distribution of the protease, which became more diffuse and less punctate (4E, F) compared to the control sample. The analyses were conducted in technical and biological triplicates, and Figure 4 displays representative images and graphs of the findings.

3.5. Soluble ADAMTS-1 is internalized by cells that do not express the nuclear protease, which start to present nuclear ADAMTS-1

To observe whether nuclear ADAMTS-1 undergoes endocytosis post-secretion, we employed HT-1080 cells that exclusively exhibit the protease in the cytoplasmic compartment (Fig 1B) and cultured these cells in a medium containing soluble ADAMTS-1. We utilized MDA-MB-231 conditioned medium, known for its nuclear ADAMTS-1 presence (Fig 1A). Control HT-1080 cells, without the conditioned medium, predominantly displayed ADAMTS-1 dispersed throughout the cytoplasm. However, upon exposure to the conditioned medium from MDA-MB-231 cells, we noted changes in the distribution and compartmentalization profile of the protease. Post-treatment, we observed increased ADAMTS-1 accumulation points in the nucleolar region, akin to that observed in MDA-MB-231 cells. These differences were found to be statistically significant (Fig 5 A, D).

To assess whether the protease's typical location in HT1080 cells could be reinstated (cytoplasmic location), we employed Dynasore, an endocytosis inhibitor known for its ability to impede the action of the dynamic protein involved in the endocytosis process. To confirm Dynasore's efficiency and rule out any non-specific inhibition, we conducted an endocytosis assay using an anti-β-integrin antibody conjugated to a red fluorophore. In Figure 5 B, the absence of Dynasore treatment (control) resulted in the endocytosis of the antibody, visible in a diffuse pattern within the cells. Conversely, in the presence of the inhibitor, β-integrin internalization did not occur, and the molecule appeared to surround the cells in the extracellular environment (white arrows). As depicted in Fig 5 C and D, treatment with 80 μM of the inhibitor failed to hinder protease endocytosis, and there was no decrease in the nucleolar localization of the protease. However, we once again observed the protease's more diffuse nuclear presence within this compartment (Fig 5 C). Analyses were performed in triplicates, both technically and biologically, with Figure 5 presenting illustrative images and graphs of the results.

To evaluate the endocytosis of ADAMTS-1, we also employed the medium conditioned by HEK-293T. HT-1080 cells were exposed to the conditioned medium secreted by the control HEK-293T cells and those expressing MPA (mcherry puromycin ADAMTS-1). As observed in supplementary figure 3A, HT-1080 cells internalized the protease, secreted by both HEK-293T and HEK293-T MPA cells, into the nuclear compartment. The number of cells exhibiting nuclear protease post-incubation with the conditioned media was higher and statistically significant (supplementary figure 3B).

3.6. The availability of ADAMTS-1 changes the migratory profile of cells.

Having observed the potential translocation of ADAMTS-1 to the nucleus/nucleolus upon conditioning HT1080 cells and fibroblasts with media secreted by MDA-MB-231 and HEK293-T MPA cells, we proceeded to assess whether this new localization could impact the cells' motility function. HT1080 cells (Fig. 6 A, B) and fibroblasts (Fig. 6 C, D) were cultured for 24 hours in conditioned media from HEK-293T MPC and HEK293T MPA cells. Treatment of HT1080 (Fig. 6 A and B) or Fibroblasts (Fig. 6 C and D) with conditioned media of HEK-293T MPA cells (supplemented with 1% fetal bovine serum) induced changes in their migratory profile compared to the control group (also supplemented with 1% fetal bovine serum), resulting in a statistically significant decrease in the cells' migratory capacity.

Analysis of the fibroblasts' migratory profile using the transwell migration assay (Figure 6 E) further revealed the influence of protease availability on the migratory pattern. Cells maintained in HEK-293T MPA conditioned medium exhibited a statistically significant reduction in fibroblast migration (Figure 6 F). Notably, the changes in cell migration (Figure 6 G) were not caused by an increase in cell proliferation or death, as indicated by the lack of statistically significant differences in the quantity of live and dead cells in the treated groups compared to the control group in the trypan blue viability assay. Hence, it can be concluded that the observed alterations in the wound assay primarily stem from the process of cell migration rather than proliferation and/or cell death. All the analysis was conducted three times each, both technically and biologically, and Figure 3 illustrates the findings.

4. Discussion

Previously, we observed ADAMTS-1 exclusively in the nucleus of breast cell lines with varying malignancy levels (15). Our findings show that epithelial phenotype cells host the protease in the nucleus, while mesenchymal phenotype cells confine it to the cytoplasm. Notably, prior evidence suggests the nuclear presence of proteases like MMP2 (28), MMP9 (29), MMP12 (30) and others (31) in nucleus, with crucial biological roles. Despite ADAMTS-1 being primarily located in the extracellular matrix (ECM) and lacking a well-defined function in the cell nucleus in the existing literature, previous studies, including Park et al.'s work on uterine epithelial cells, have highlighted its presence in the nuclei (32). These proteases may serve as chromatin remodelers, impacting nuclear matrix structure, apoptosis, and cell proliferation regulation (28). Studies suggest that proteins within the nuclear matrix share functional traits with those in the ECM, aiding in the anchoring of diverse molecules (20). For example, Ren et al. (2017) demonstrated ADAMTS-4's nuclear translocation, where it interacts with and cleaves PARP-1, directly triggering apoptosis (33). At the same time, studies demonstrated that ADAMTS1 inhibits angiogenesis both in vitro and in vivo, suggesting its role in inducing endothelial cell apoptosis. Notably, the inhibition of proliferation was observed specifically in endothelial cells, and not in other cell types, including smooth muscle cells, fibroblasts, and CHO-K1 cells (Chinese hamster ovary cell) (34). Both ADAMTS-1 and 4 share the fundamental protein structure typical of this family, differing only in the former's possession of two thrombospondin domains in the C-terminal region (1). Despite this dissimilarity, as both are aggrecanases, they may function similarly

within the nucleus. Prior evidence has shown ADAMTS-1's cleavage activity within breast cell nuclei, indicating its potential for remodeling the nuclear matrix, given the presence of ADAMTS substrates like Aggrecan (15) and Versican(16) in the nucleus. Importantly, it is worth noting that ADAMTS-1 can be activated through auto-cleavage or furin activity, which is present in the nucleus (35).

Our study has shown that ADAMTS-1 is linked with nuclear structures but not chromatin. By impeding vesicle secretion with Monensin, the protease's localization underwent changes. Monensin possesses the capacity to induce functional and morphological alterations in the Golgi apparatus and mitochondria (36–38), with effects fully reversible after 24 hours of treatment (39). Our results suggest that Monensin disrupted the Golgi apparatus, thus hindering ADAMTS-1's secretion into the extracellular environment and its subsequent localization within the cell nucleus. This implies that the protease necessitates secretion before internalizing into the nucleus. To assess ADAMTS-1's nucleus/cytoplasmic translocation, we employed a selective inhibitor of nuclear transport via importin β (40, 41). Despite incubation with importazole, ADAMTS-1 continued to localize within the nucleus. As a positive control, we utilized LPS (lipopolysaccharide) (42, 43), a known inducer of inflammatory cytokines, such as the transcription factor NF-ƙB (44). When inactive, NF-ƙB remains in the cytoplasm, bound to an inhibitory protein called IƙB, preventing its translocation to the nucleus (42, 43). However, upon LPS stimulation, IƙB undergoes phosphorylation and degradation, triggering NF-ƙB's translocation to the nucleus (45).

No literature reports the presence of the typical nuclear localization signal (NLS) in ADAMTS-1. The NLS, a short sequence of amino acids, facilitates protein transport to the nucleus through importin receptors (46). The absence of this NLS in ADAMTS-1 aligns with the Importazole experiment results, as proteins without the classical NLS employ alternative importins for transport. Recent studies have identified the specific NLS sequence in Matrix Metalloproteinase (MMP) proteins, known for their association with cancer and neurological disorders (47). Significantly, the NLS sequence has been identified in ADAMTS-13, a protein conventionally recognized as a secreted metalloprotease, suggesting potential additional biological functions (48). Hunt et al. noted the presence of a cluster of positively charged amino acid residues at the distal end of the ADAMTS13 propeptide, bearing striking similarities to the K-K/R-X-K/R monopartite NLSs (49). Furthermore, the maturation process of ADAMTS-1 involves two distinct processing events, resulting in the release of two forms of the protein - an 87 kDa active form and a 65 kDa soluble form after specific cleavage events (14). Our studies revealed that the administration of monensin inhibits the nuclear entry of ADAMTS-1 65 kDa. This suggests that it possibly needs to be secreted for processing in the extracellular matrix by furins and other molecules, before returning to the nucleus. While the full-length ADAMTS-4 weighs 90 kDa, its 68 kDa form was found to be responsible for PARP-1 cleavage, triggering cell apoptosis. This implies that this protease also requires processing prior to its entry into the nucleus (33).

Our findings show that heparin modifies the compartmentalization of ADAMTS-1, elevating its expression in the extracellular medium while leaving the intracellular expression unaffected. Literature reports suggest that heparin hinders the endocytosis of MMP13 by disrupting the interaction between MMP13 and the LRP1 receptor (receptor-related protein

1), which facilitates the molecule's internalization (50). Furthermore, heparin binds to both ADAMTS-4 and ADAMTS-5 (51, 52), hindering the endocytosis of these molecules. Furthermore, Liu et al. (2016) demonstrated, using TA3 murine mammary carcinoma cells, that the cleavage of ADAMTS-1 is hindered by heparin (53). Heparin, a negatively charged and sulfated molecule, interacts with various amino acid residues in proteins, owing to its distinctive properties, and can exhibit an affinity for multiple proteins simultaneously. In a microenvironment characterized by a high abundance of heparin, ADAMTS-1 binds to it through its spacer/Cysrich region. This binding protects the region from proteolytic cleavage, thus maintaining ADAMTS-1 in its full-length form, enabling it to effectively bind and cleave its substrates (53).

Our study revealed the absence of nuclear ADAMTS-1 in mesenchymal-origin cells. Consequently, we exposed HT-1080 and fibroblasts (cytoplasmic proteases) to conditioned medium secreted by MDA-MB-231 and HEK-293T (nuclear proteases), leading to the appearance of the protease in the nucleus. Based on our results, we propose that the soluble protease in this conditioned medium undergoes endocytosis by mesenchymal-origin cells. Literature studies indicate that tumor cells can adopt epithelial-like traits, as demonstrated by Casal et al., wherein increased ADAMTS-1 expression in mesenchymal-origin cells contributes to tumor plasticity and the acquisition of epithelial characteristics (54).

Furthermore, our research suggests that the internalization of ADAMTS-1 by mesenchymal cells does not follow the classical endocytosis pathway mediated by plasma membrane protein fusion, as the dynamin inhibitor failed to prevent the protease's entry. Dynamin inhibition, along with other regulators of cellular trafficking, represents potent tools for effectively blocking endocytosis (55, 56). Recent reports have identified ADAMTS1 as a low-density lipoprotein receptor-related protein 1 (LRP1) (57). Studies have revealed that ADAMTS-4, sharing a close structural resemblance to ADAMTS-1, is endocytosed by chondrocytes through LRP1, thereby allowing it to become accessible inside the cell (58).

By taking over this nuclear compartment, ADAMTS-1 can effectively modify the functional profile of these cells. Existing literature consistently demonstrates that ADAMTS-1 impacts cell migration, with increased protease availability in the extracellular medium correlating with reduced migratory potential (59, 60). Comparing this insight with our findings, we propose that ADAMTS-1, upon translocating to the nucleus, can similarly influence cellular motility processes. In the case of invasive breast cancer cells (MDA-MB-231), the absence of ADAMTS-1 triggers heightened migratory activity in the lineage (60), while our observations reveal well-characterized ADAMTS-1 in the nucleus of these cells (15). Evidence supports an intracellular role for versican in vascular cells, where it seems to participate in mitotic spindle organization during cell division, acting as a known ADAMTS-1 substrate (16). Thus, ADAMTS-1 likely participates in the cleavage of versican within the nucleus.

A study has shown an increase in MMP-2 and -9 within neuron nuclei during the initial post-ischemic reperfusion phase, observed in both human stroke cases and animal models. These gelatinases bound to the nucleus contribute to oxidative DNA damage by degrading nuclear matrix proteins, such as PARP-1 and XRCC1, impairing their ability to repair DNA

lesions caused by post-stroke oxidative stress. Given ADAMTS-1's elevated expression under hypoxic conditions, it might play a similar role (35).

Further studies are required to provide fresh insights into the transport and trafficking of ADAMTS-1, along with the identification of new interaction partners. Future investigations aim to elucidate the precise mechanisms by which ADAMTS-1 accesses the cell nucleus, recognizes, and cleaves other components within the cell nucleus.

5. Conclusion

Based on our findings, we can deduce that nuclear ADAMTS-1 expression differs between cells derived from epithelial and mesenchymal origins. Moreover, the localization of ADAMTS-1 underwent changes when we disrupted the functional secretion of cells through the Golgi Apparatus. Mesenchymal cells cultured in an ADAMTS-1-enriched medium exhibited nuclear localization of the protease, which did not occur through clathrin-mediated endocytosis. Furthermore, the nucleocytoplasmic transport of the protease proved to be independent of the classic importin-β protein. Additionally, we demonstrated that increased ADAMTS-1 availability diminishes the migratory capacity of cells. Figure 7 presents a summary of the collected data.

Supplementary Material

Refer to Web version on PubMed Central for supplementary material.

Acknowledgments

We thank Professor Ruy Jaeger for making the fluorescence microscope available in his laboratory. Thanks to Heydi Noriega for developing the HEK293T MPA/MPC cell line. We express our gratitude to Professor Juan Carlos Rodríguez-Manzaneque for providing the HT1080 ATS1 and Z11 cell lines. Thanks to funding agencies: State of São Paulo Research Foundation and National Institutes of Health grant.

Funding:

This investigation was supported by the State of São Paulo Research Foundation (FAPESP grants 2018/05566-6, 2015/09845-9); and National Institutes of Health grant (R35GM136226).Ministry of Science and Innovation from the Government of Spain (PID2019-104416RB-I00) to J.C.R.-M.

Data availability

Data will be made available on request.

References

1. Kelwick R, Desanlis I, Wheeler GN, Edwards DR. The ADAMTS (A Disintegrin and Metalloproteinase with Thrombospondin motifs) family. Genome Biol. 2015;16:113. [PubMed: 26025392]
2. Porter S, Clark IM, Kevorkian L, Edwards DR. The ADAMTS metalloproteinases. Biochem J. 2005;386(Pt 1):15–27. [PubMed: 15554875]
3. Stanton H, Melrose J, Little CB, Fosang AJ. Proteoglycan degradation by the ADAMTS family of proteinases. Biochim Biophys Acta. 2011;1812(12):1616–29. [PubMed: 21914474]
4. Thai SN, Iruela-Arispe ML. Expression of ADAMTS1 during murine development. Mech Dev. 2002;115(1–2):181–5. [PubMed: 12049787]

5. Salter RC, Ashlin TG, Kwan AP, Ramji DP. ADAMTS proteases: key roles in atherosclerosis? J Mol Med (Berl). 2010;88(12):1203–11. [PubMed: 20652528]
6. Russell DL, Brown HM, Dunning KR. ADAMTS proteases in fertility. Matrix Biol. 2015;44–46:54–63.
7. Dubail J, Apte SS. Insights on ADAMTS proteases and ADAMTS-like proteins from mammalian genetics. Matrix Biol. 2015;44–46:24–37.
8. Güneş MF, Akpinar MB, Cömertoğlu I, Akyol S, Demirçelik B, Gürel Ö, et al. The Investigation of a Disintegrin and Metalloproteinase with ThromboSpondin Motifs (ADAMTS) 1, 5 and 16 in Thoracic Aortic Aneurysms and Dissections. Clin Lab. 2016;62(3):425–33. [PubMed: 27156333]
9. Kuno K, Matsushima K. ADAMTS-1 protein anchors at the extracellular matrix through the thrombospondin type I motifs and its spacing region. J Biol Chem. 1998;273(22):13912–7. [PubMed: 9593739]
10. Porter S, Scott SD, Sassoon EM, Williams MR, Jones JL, Girling AC, et al. Dysregulated expression of adamalysin-thrombospondin genes in human breast carcinoma. Clin Cancer Res. 2004;10(7):2429–40. [PubMed: 15073121]
11. Fernández-Rodríguez R, Rodríguez-Baena FJ, Martino-Echarri E, Peris-Torres C, Del Carmen Plaza-Calonge M, Rodríguez-Manzaneque JC. Stroma-derived but not tumor ADAMTS1 is a main driver of tumor growth and metastasis. Oncotarget. 2016;7(23):34507–19. [PubMed: 27120788]
12. Kuno K, Kanada N, Nakashima E, Fujiki F, Ichimura F, Matsushima K. Molecular cloning of a gene encoding a new type of metalloproteinase-disintegrin family protein with thrombospondin motifs as an inflammation associated gene. J Biol Chem. 1997;272(1):556–62. [PubMed: 8995297]
13. Kuno K, Bannai K, Hakozaki M, Matsushima K, Hirose K. The carboxyl-terminal half region of ADAMTS-1 suppresses both tumorigenicity and experimental tumor metastatic potential. Biochem Biophys Res Commun. 2004;319(4):1327–33. [PubMed: 15194513]
14. Longpré JM, Leduc R. Identification of prodomain determinants involved in ADAMTS-1 biosynthesis. J Biol Chem. 2004;279(32):33237–45. [PubMed: 15184385]
15. Silva SV, Lima MA, Cella N, Jaeger RG, Freitas VM. ADAMTS-1 Is Found in the Nuclei of Normal and Tumoral Breast Cells. PLoS One. 2016;11(10):e0165061. [PubMed: 27764205]
16. Carthy JM, Abraham T, Meredith AJ, Boroomand S, McManus BM. Versican localizes to the nucleus in proliferating mesenchymal cells. Cardiovasc Pathol. 2015;24(6):368–74. [PubMed: 26395512]
17. Si-Tayeb K, Monvoisin A, Mazzocco C, Lepreux S, Decossas M, Cubel G, et al. Matrix metalloproteinase 3 is present in the cell nucleus and is involved in apoptosis. Am J Pathol. 2006;169(4):1390–401. [PubMed: 17003494]
18. Si-Yayeb K, Monvoisin A, Mazzocco C, Lépreux S and Rosenbaum J. Unexpected localization of the matrix metalloproteinase-3 (MMP-3) within the cell nucleus in liver cancer cells. Mechanisms and consequences. Journal of Hepatology. 2003;38:105.
19. Ritter LM, Garfield SH, Thorgeirsson UP. Tissue inhibitor of metalloproteinases-1 (TIMP-1) binds to the cell surface and translocates to the nucleus of human MCF-7 breast carcinoma cells. Biochem Biophys Res Commun. 1999;257(2):494–9. [PubMed: 10198240]
20. Kwan JA, Schulze CJ, Wang W, Leon H, Sariahmetoglu M, Sung M, et al. Matrix metalloproteinase-2 (MMP-2) is present in the nucleus of cardiac myocytes and is capable of cleaving poly (ADP-ribose) polymerase (PARP) in vitro. FASEB J. 2004;18(6):690–2. [PubMed: 14766804]
21. Morales J, Li L, Fattah FJ, Dong Y, Bey EA, Patel M, et al. Review of poly (ADP-ribose) polymerase (PARP) mechanisms of action and rationale for targeting in cancer and other diseases. Crit Rev Eukaryot Gene Expr. 2014;24(1):15–28. [PubMed: 24579667]
22. Apte SS. A disintegrin-like and metalloprotease (reprolysin type) with thrombospondin type 1 motifs: the ADAMTS family. Int J Biochem Cell Biol. 2004;36(6):981–5. [PubMed: 15094112]
23. Silva TA, Smuczek B, Valadão IC, Dzik LM, Iglesia RP, Cruz MC, et al. AHNAK enables mammary carcinoma cells to produce extracellular vesicles that increase neighboring fibroblast cell motility. Oncotarget. 2016;7(31):49998–50016. [PubMed: 27374178]

24. Rodríguez-Manzaneque JC, Westling J, Thai SN, Luque A, Knauper V, Murphy G, et al. ADAMTS1 cleaves aggrecan at multiple sites and is differentially inhibited by metalloproteinase inhibitors. Biochem Biophys Res Commun. 2002;293(1):501–8. [PubMed: 12054629]
25. Noriega-Guerra H, Cruz MC, Ribeiro PRL, Strnadel J, Wang H, Klemke RL, et al. ADAMTS-1 disrupts HGF/c-MET signaling and HGF-stimulated cellular processes in fibrosarcoma. Exp Cell Res. 2018;363(2):271–82. [PubMed: 29355494]
26. Shaw G, Morse S, Ararat M, Graham FL. Preferential transformation of human neuronal cells by human adenoviruses and the origin of HEK 293 cells. FASEB J. 2002;16(8):869–71. [PubMed: 11967234]
27. Preta G, Cronin JG, Sheldon IM. Dynasore - not just a dynamin inhibitor. Cell Commun Signal. 2015;13:24. [PubMed: 25889964]
28. Sinha SK, Asotra K, Uzui H, Nagwani S, Mishra V, Rajavashisth TB. Nuclear localization of catalytically active MMP-2 in endothelial cells and neurons. Am J Transl Res. 2014;6(2):155–62. [PubMed: 24489995]
29. Zimowska M, Swierczynska M, Ciemerych MA. Nuclear MMP-9 role in the regulation of rat skeletal myoblasts proliferation. Biol Cell. 2013;105(8):334–44. [PubMed: 23646930]
30. Mouton AJ, Rivera Gonzalez OJ, Kaminski AR, Moore ET, Lindsey ML. Matrix metalloproteinase-12 as an endogenous resolution promoting factor following myocardial infarction. Pharmacol Res. 2018;137:252–8. [PubMed: 30394317]
31. Mannello F, Medda V. Nuclear localization of matrix metalloproteinases. Prog Histochem Cytochem. 2012;47(1):27–58. [PubMed: 22226510]
32. Park M, Park SH, Park H, Kim HR, Lim HJ, Song H. ADAMTS-1: a novel target gene of an estrogen-induced transcription factor, EGR1, critical for embryo implantation in the mouse uterus. Cell Biosci. 2021;11(1):155. [PubMed: 34348778]
33. Ren P, Hughes M, Krishnamoorthy S, Zou S, Zhang L, Wu D, et al. Critical Role of ADAMTS-4 in the Development of Sporadic Aortic Aneurysm and Dissection in Mice. Sci Rep. 2017;7(1):12351. [PubMed: 28955046]
34. Obika M, Ogawa H, Takahashi K, Li J, Hatipoglu OF, Cilek MZ, et al. Tumor growth inhibitory effect of ADAMTS1 is accompanied by the inhibition of tumor angiogenesis. Cancer Sci. 2012;103(10):1889–97. [PubMed: 22776012]
35. Yang Y, Candelario-Jalil E, Thompson JF, Cuadrado E, Estrada EY, Rosell A, et al. Increased intranuclear matrix metalloproteinase activity in neurons interferes with oxidative DNA repair in focal cerebral ischemia. J Neurochem. 2010;112(1):134–49. [PubMed: 19840223]
36. Souza AC, Machado FS, Celes MR, Faria G, Rocha LB, Silva JS, et al. Mitochondrial damage as an early event of monensin-induced cell injury in cultured fibroblasts L929. J Vet Med A Physiol Pathol Clin Med. 2005;52(5):230–7. [PubMed: 15943607]
37. Kato S, Chen J, Cornog KH, Zhang H, Roberts JD. The Golgi apparatus regulates cGMP-dependent protein kinase I compartmentation and proteolysis. Am J Physiol Cell Physiol. 2015;308(11):C944–58. [PubMed: 25855081]
38. Charvat RA, Arrizabalaga G. Oxidative stress generated during monensin treatment contributes to altered Toxoplasma gondii mitochondrial function. Sci Rep. 2016;6:22997. [PubMed: 26976749]
39. Lavine MD, Arrizabalaga G. Analysis of monensin sensitivity in Toxoplasma gondii reveals autophagy as a mechanism for drug induced death. PLoS One. 2012;7(7):e42107. [PubMed: 22848721]
40. Soderholm JF, Bird SL, Kalab P, Sampathkumar Y, Hasegawa K, Uehara-Bingen M, et al. Importazole, a small molecule inhibitor of the transport receptor importin-β. ACS Chem Biol. 2011;6(7):700–8. [PubMed: 21469738]
41. Zhu ZC, Liu JW, Li K, Zheng J, Xiong ZQ. KPNB1 inhibition disrupts proteostasis and triggers unfolded protein response-mediated apoptosis in glioblastoma cells. Oncogene. 2018;37(22):2936–52. [PubMed: 29520102]
42. Kublun I, Ehm P, Brehm MA, Nalaskowski MM. Efficacious inhibition of Importin α/β-mediated nuclear import of human inositol phosphate multikinase. Biochimie. 2014;102:117–23. [PubMed: 24632208]

43. Mahipal A, Malafa M. Importins and exportins as therapeutic targets in cancer. Pharmacol Ther. 2016;164:135–43. [PubMed: 27113410]
44. Andreakos E, Sacre SM, Smith C, Lundberg A, Kiriakidis S, Stonehouse T, et al. Distinct pathways of LPS-induced NF-kappa B activation and cytokine production in human myeloid and nonmyeloid cells defined by selective utilization of MyD88 and Mal/TIRAP. Blood. 2004;103(6):2229–37. [PubMed: 14630816]
45. Siebenlist U NF kappa B/I kappa B proteins. Their role in cell growth, differentiation and development. Madrid, Spain, July 7–10, 1996. Biochim Biophys Acta. 1997;1332(1):R7–13. [PubMed: 9061013]
46. Cokol M, Nair R, Rost B. Finding nuclear localization signals. EMBO Rep. 2000;1(5):411–5. [PubMed: 11258480]
47. Abdukhakimova D, Xie Y. Comparative Analysis of NLS Sequence Suggests the Evolutionary Origin of Nuclear Matrix Metalloproteinase 7 during Cancer Evolution. Int. J. Pharma Med. Biol. Sci; 2016. p. 206 – 10.
48. Hunt RC, Geetha S, Allen CE, Hershko K, Fathke R, Kong PL, et al. Detection of a secreted metalloprotease within the nuclei of liver cells. Mol Biosyst. 2011;7(6):2012–8. [PubMed: 21479334]
49. Chelsky D, Ralph R, Jonak G. Sequence requirements for synthetic peptide-mediated translocation to the nucleus. Mol Cell Biol. 1989;9(6):2487–92. [PubMed: 2668735]
50. Yamamoto K, Okano H, Miyagawa W, Visse R, Shitomi Y, Santamaria S, et al. MMP-13 is constitutively produced in human chondrocytes and co-endocytosed with ADAMTS-5 and TIMP-3 by the endocytic receptor LRP1. Matrix Biol. 2016;56:57–73. [PubMed: 27084377]
51. Zeng W, Corcoran C, Collins-Racie LA, Lavallie ER, Morris EA, Flannery CR. Glycosaminoglycan-binding properties and aggrecanase activities of truncated ADAMTSs: comparative analyses with ADAMTS-5, −9, −16 and −18. Biochim Biophys Acta. 2006;1760(3):517–24. [PubMed: 16507336]
52. Flannery CR, Zeng W, Corcoran C, Collins-Racie LA, Chockalingam PS, Hebert T, et al. Autocatalytic cleavage of ADAMTS-4 (Aggrecanase-1) reveals multiple glycosaminoglycan-binding sites. J Biol Chem. 2002;277(45):42775–80. [PubMed: 12202483]
53. Liu YJ, Xu Y, Yu Q. Full-length ADAMTS-1 and the ADAMTS-1 fragments display pro- and antimetastatic activity, respectively. Oncogene. 2006;25(17):2452–67. [PubMed: 16314835]
54. Casal C, Torres-Collado AX, Plaza-Calonge MeC, Martino-Echarri E, Ramón Y Cajal S, Rojo F, et al. ADAMTS1 contributes to the acquisition of an endothelial-like phenotype in plastic tumor cells. Cancer Res. 2010;70(11):4676–86. [PubMed: 20484033]
55. Ivanov AI. Pharmacological inhibitors of exocytosis and endocytosis: novel bullets for old targets. Methods Mol Biol. 2014;1174:3–18. [PubMed: 24947371]
56. Basagiannis D, Zografou S, Galanopoulou K, Christoforidis S. Dynasore impairs VEGFR2 signalling in an endocytosis-independent manner. Sci Rep. 2017;7:45035. [PubMed: 28327657]
57. Yamamoto K, Scavenius C, Meschis MM, Gremida AME, Mogensen EH, Thøgersen IB, et al. A top-down approach to uncover the hidden ligandome of low-density lipoprotein receptor-related protein 1 in cartilage. Matrix Biol. 2022;112:190–218. [PubMed: 36028175]
58. Yamamoto K, Troeberg L, Scilabra SD, Pelosi M, Murphy CL, Strickland DK, et al. LRP-1-mediated endocytosis regulates extracellular activity of ADAMTS-5 in articular cartilage. FASEB J. 2013;27(2):511–21. [PubMed: 23064555]
59. de Assis Lima M, da Silva SV, Serrano-Garrido O, Hülsemann M, Santos-Neres L, Rodríguez-Manzaneque JC, et al. Metalloprotease ADAMTS-1 decreases cell migration and invasion modulating the spatiotemporal dynamics of Cdc42 activity. Cell Signal. 2021;77:109827. [PubMed: 33161094]
60. Freitas VM, do Amaral JB, Silva TA, Santos ES, Mangone FR, Pinheiro JeJ, et al. Decreased expression of ADAMTS-1 in human breast tumors stimulates migration and invasion. Mol Cancer. 2013;12:2. [PubMed: 23289900]

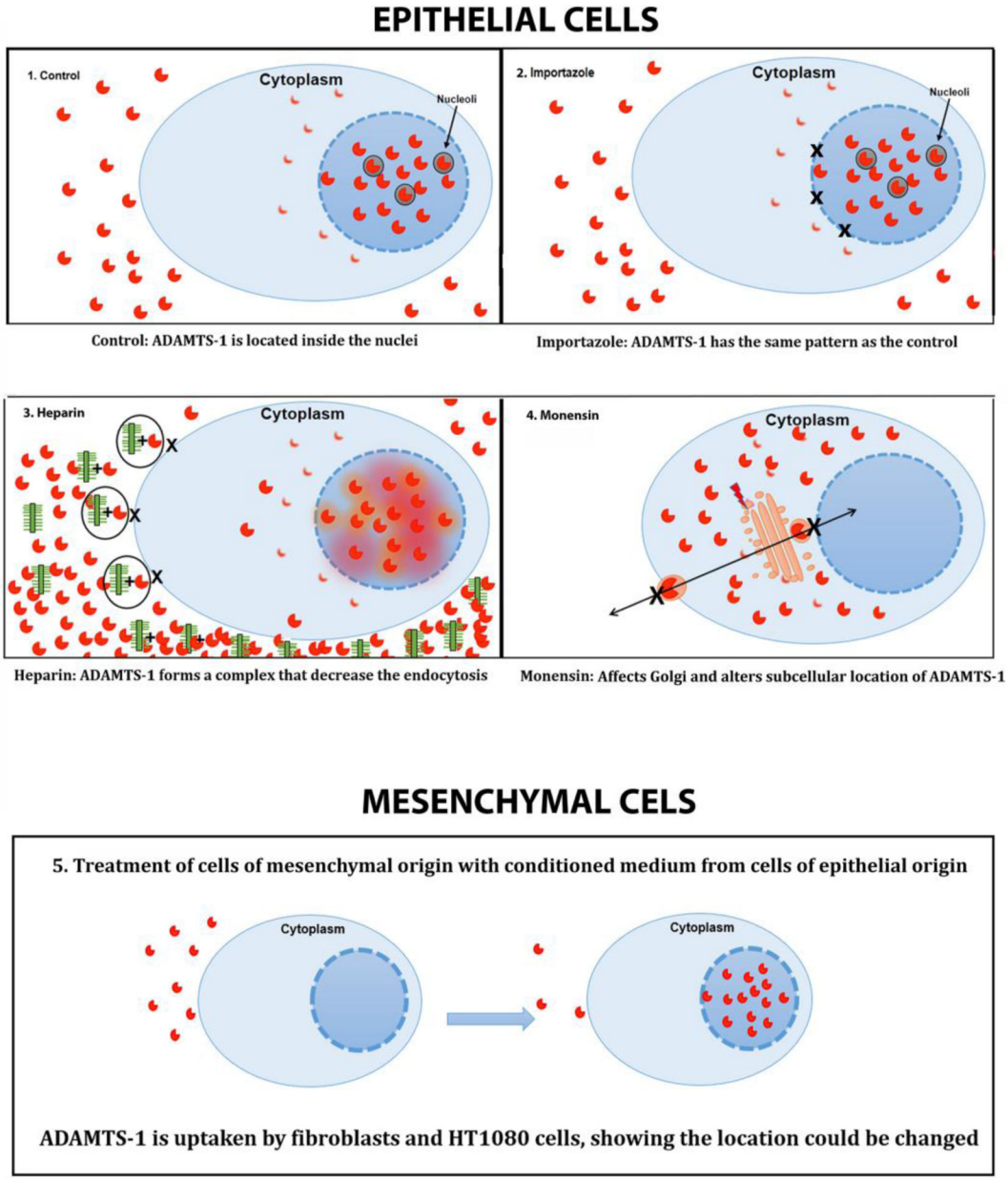

Fig 1. ADAMTS-1 is in the nucleus of cells of epithelial origin, but in cells of mesenchymal origin its distribution is cytoplasmic.

Immunofluorescence analysis in (A) epithelial-origin cells (HTR-8; MDAH-2774; NIH-OVCAR-3; MDA-MB-231) and (B) mesenchymal-origin cells (Fibroblast; HT1080; MuM-2B) clearly illustrates this distinct compartmentalization of ADAMTS-1. Blue:Core, Green:F-actin and Red:ADAMTS-1. Scale bar: 5 μm epithelial-origin cells/20 μm mesenchymal-origin cells. Experiments were conducted in biological and experimental triplicates (N=3).

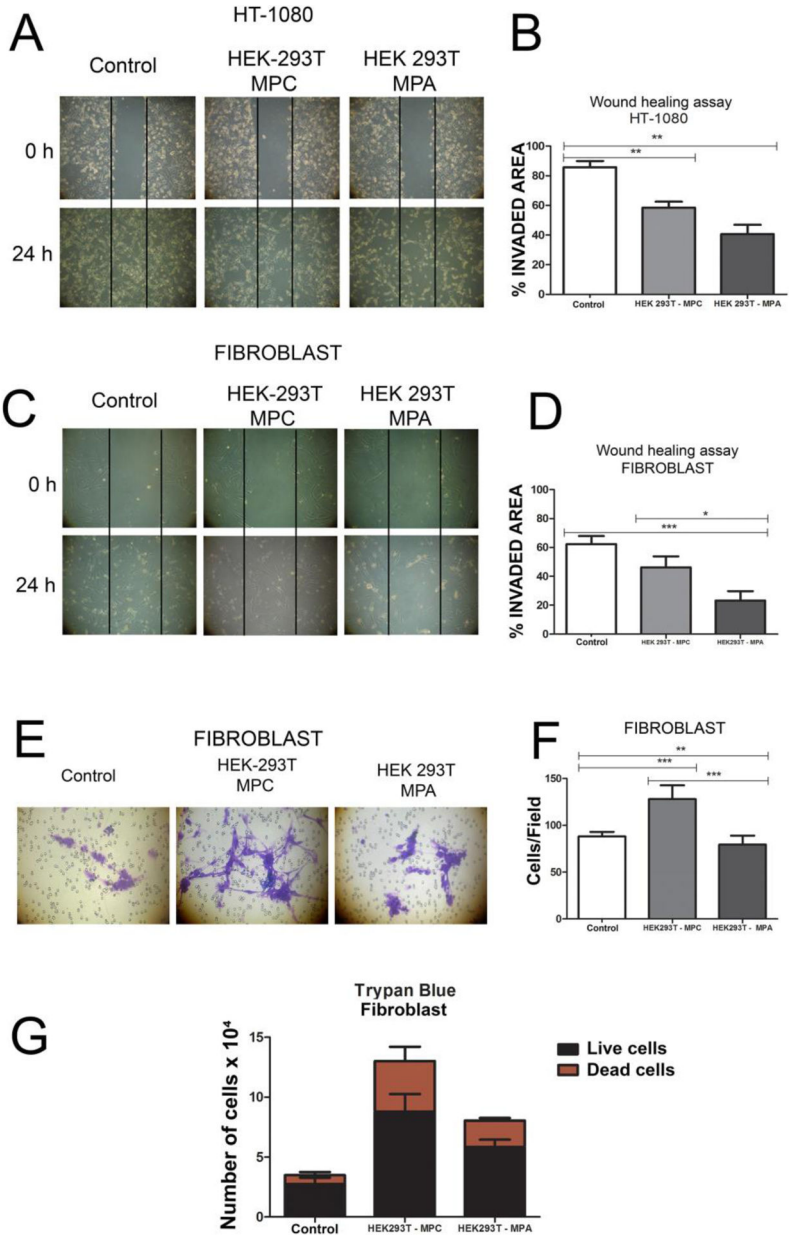

Fig 2. ADAMTS-1 is a protease linked to nuclear structures of MDA-MB-231 cells.

Conducting subcellular fractionation on coverslips involved incubating cells with various buffers containing different concentrations of salts and DNAse. This process aimed to assess the presence of ADAMTS-1 and histone, the latter serving as a positive control for DNAse activity. Immunolocalization of ADAMTS-1 and Histone H1 in MDA-MB-231 cells confirms that ADAMTS-1 exhibits a robust association with nuclear structures. Blue:Core; Green:F-actin; Red:ADAMTS-1 or Histone. Scale bar: 5μm. Experiments were conducted in biological and experimental triplicates (N=3).

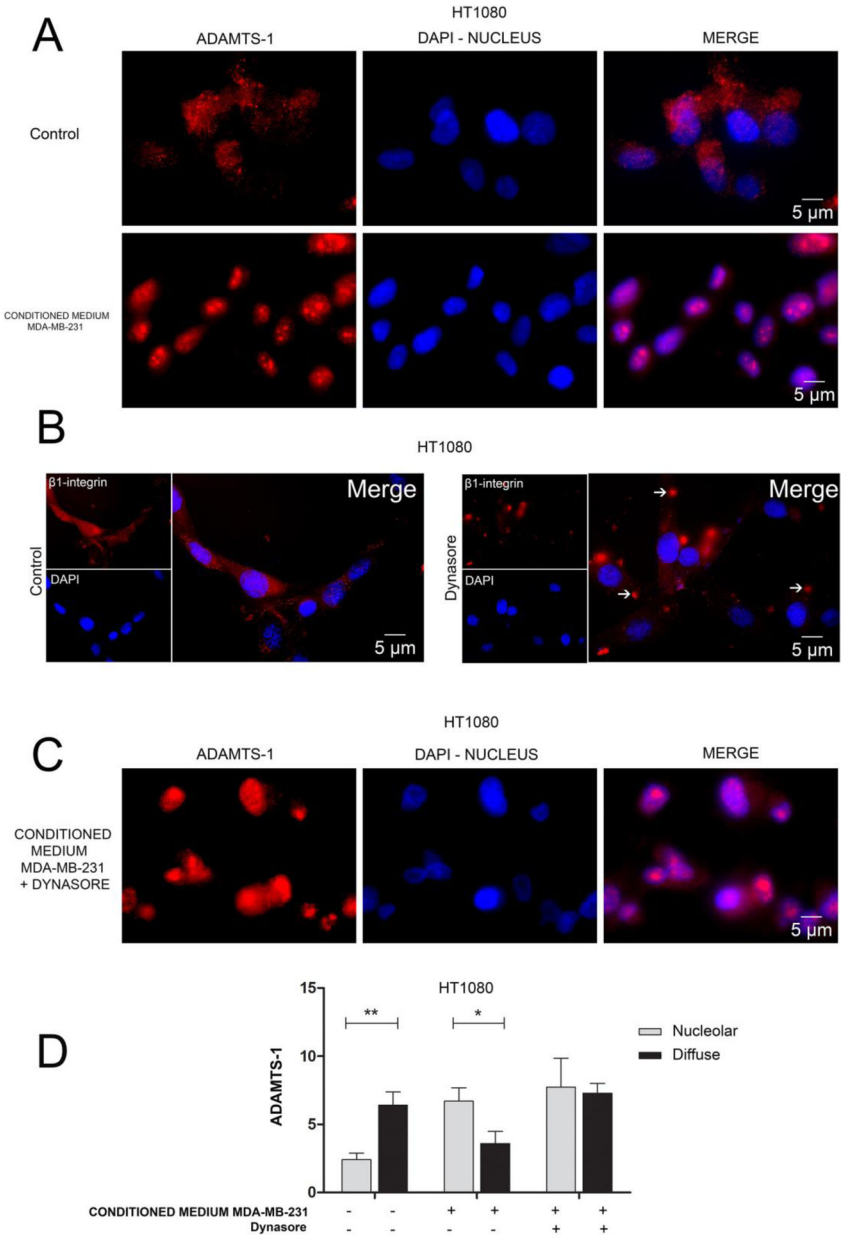

Fig 3. Importing ADAMTS-1 into the core does not use Importin and the Golgi apparatus is involved in the compartmentalization of the nuclear protease.

Following a 24-hour treatment of MDA-MB-231 cells with 2 µM Monensin in a 10% FBS culture medium, the localization of the protease was assessed using both Immunofluorescence and Western Blot analysis of cell fractions. The Immunofluorescence images (A, B) illustrate notable changes in the distribution pattern of ADAMTS-1 within cells exposed to Monensin. Furthermore, the protein analysis (C) revealed an increase in cytoplasmic ADAMTS-1 levels upon treatment, coupled with a reduction in protease secretion (C - Control; M - Monensin-treated). In a separate experiment, MDA-MB-231 cells were treated with 50 µM Importazole for 5 hours, followed by a 1-hour exposure to 1ug/ml of LPS, and subsequently analyzed via Immunofluorescence (D, E). Blue:Core,

Green:F-actin and Red:ADAMTS-1/Golgina 97/NFκB. Scale bar: 5μm. Experiments were conducted in biological and experimental triplicates (N=3).

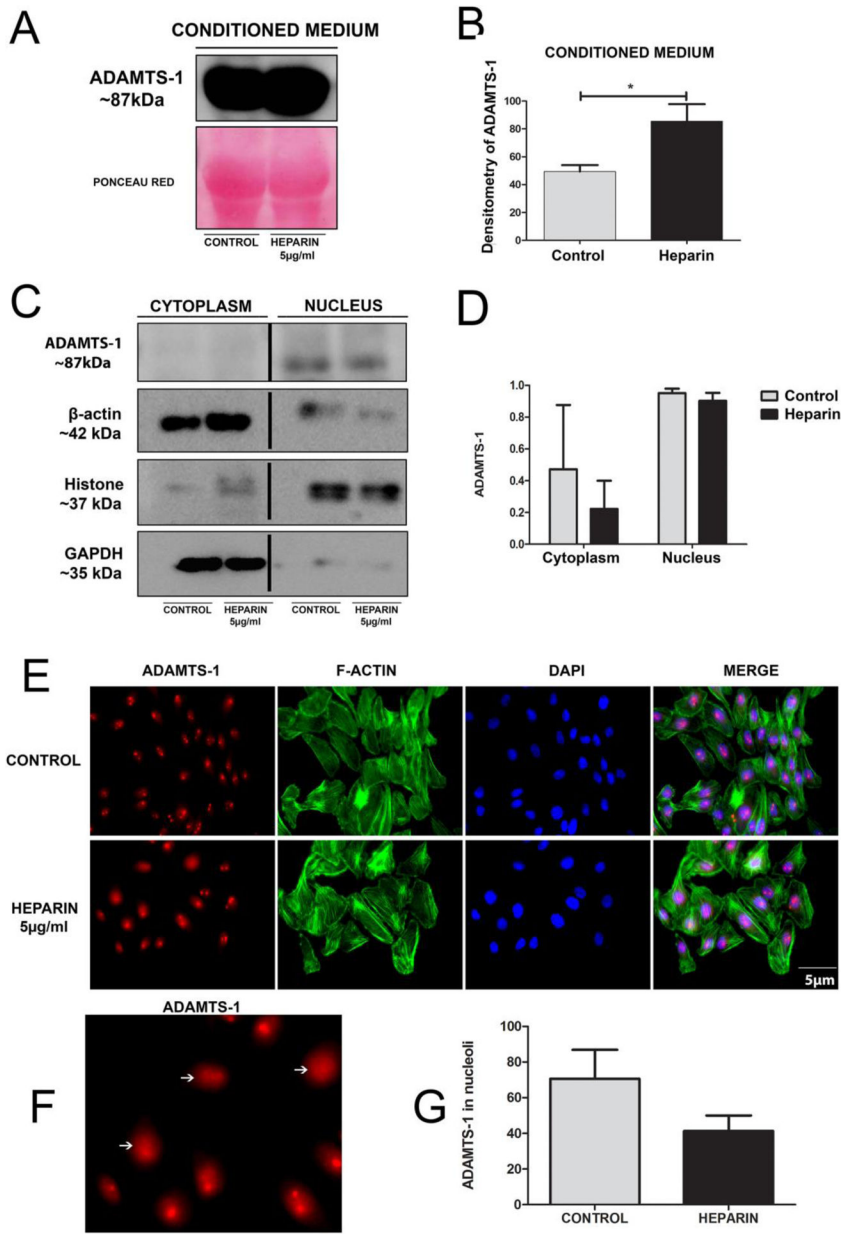

Fig 4. Heparin alters the ADAMTS-1 secretion profile, but not the amount of nuclear ADAMTS-1.

The Western blot analysis depicted (A) the conditioned medium, (C) as well as the cytoplasmic and nuclear fractions obtained from MDA-MB231 cells treated with 5 µg/ml for 24 hours. A representative graph of the conditioned medium (B) and the cytoplasm and nucleus (D) revealed statistically significant differences between groups ($p \leq 0.05$). Moreover, Immunofluorescence images (E) demonstrated the distribution pattern of ADAMTS-1 in Heparin-treated cells compared to the control sample, with an insert (F) highlighting the discernibly altered distribution pattern in the treated cells. Additionally, a representative graph (G) illustrated the presence of ADAMTS-1 in the nucleus of both control and heparin-treated MDA-MB231 cells. Blue:Core, Green:F-actin and Red-

ADAMTS-1. Scale bar: 5μm. Experiments were conducted in biological and experimental triplicates (N=3).

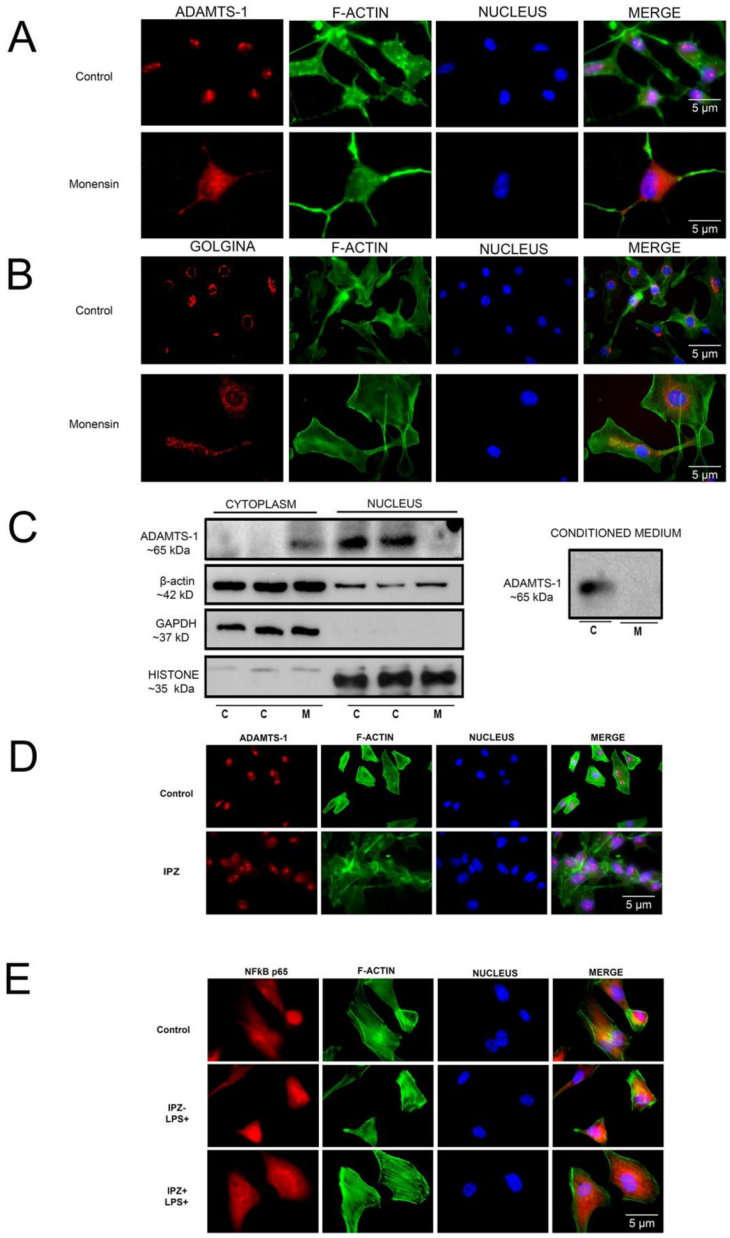

Fig 5. ADAMTS-1 is internalized by cells of mesenchymal origin and they start to present nuclear ADAMTS-1, and blocking endocytosis partially prevents the presence of the protease in the nucleus.

HT1080 cells underwent a 24-hour treatment with the conditioned medium secreted by MDA-MB-231 cells, followed by immunofluorescence analysis as shown in (A), with the upper panel depicting control cells and the lower panel representing cells treated with MDA-MB-231 conditioned medium. Subsequently, (B) illustrates HT1080 cells incubated with β1 integrin conjugated to Alexa fluor 568, without Dynasore (left panel) and with Dynasore (right panel). In (C), HT1080 cells were maintained in conditioned medium secreted by MDA-MB-231 cells, along with 80 µM Dynasore. The results of the experiments depicted in A and C are summarized in (D), which presents a graph displaying the number of cells with the protease located in the nucleolar region (dots). Statistically significant differences

between groups were denoted as *p≥0.05, **p≥0.005, and ***p≥0.0005. Blue:Core and Red:ADAMTS-1 and β-integrin. Scale bar: 5μm. Experiments were conducted in biological and experimental triplicates(N=3).

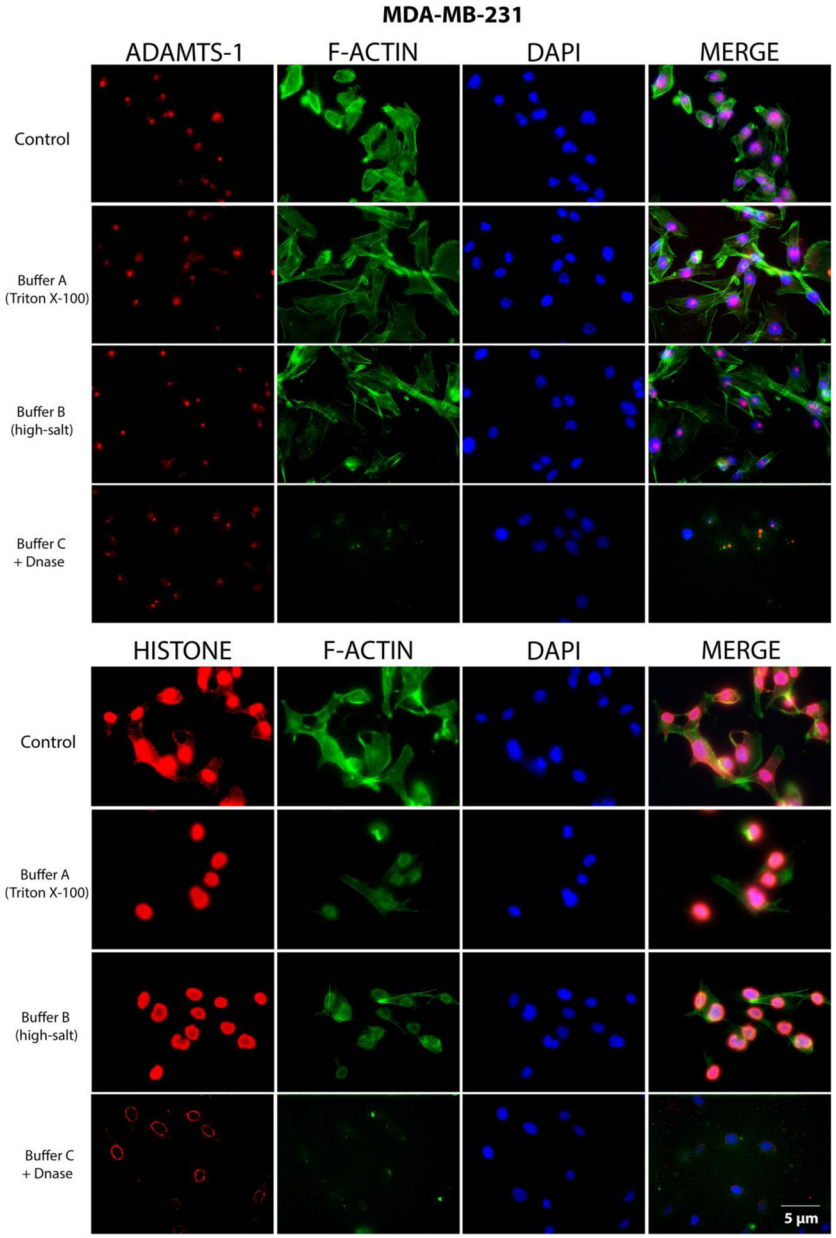

Fig 6. Increased availability of ADAMTS-1 decreases cell motility.

(A, B) HT1080 and (C, D) fibroblasts were treated with HEK293-T (MPC) and HEK293-T MPA culture media and later we evaluated the migratory behavior of these cells by the "wound healing assay" method and also (E, F) the migratory behavior of fibroblasts was evaluated by transwell migration assay. (G) Cell viability test by the Trypan Blue exclusion method. Differences between groups were considered statistically significant when *p≥0.05, **p≥0.005 and ***p≥0.0005. Experiments were conducted in biological and experimental triplicates (N=3).

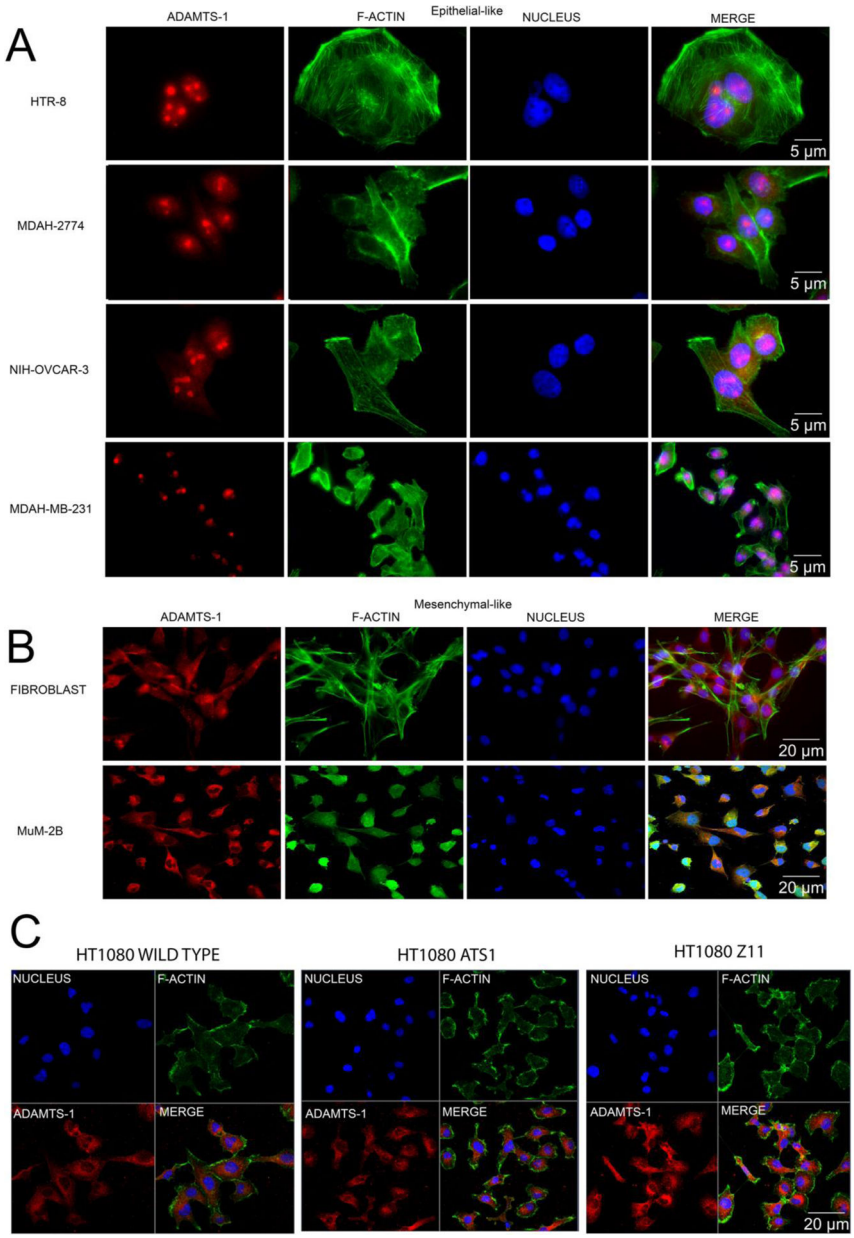

Figure 7. Summary of the obtained results.

1. It was observed that ADAMTS-1 exhibits nuclear localization in epithelial cells. 2. Upon treatment with Importazole, an inhibitor of the importin-β receptor transport, ADAMTS-1 remained confined within the nucleus. 3. The introduction of heparin, which prevents protease cleavage, resulted in a more diffused pattern of ADAMTS-1 within the nucleus. 4. Treatment with Monensin, wich disrupts the Golgi apparatus, hindered ADAMTS-1 from entering the nucleus, leaving it confined within the cytoplasm. 5. When mesenchymal cells were exposed to conditioned medium from epithelial cells, they were able to absorb and allocate ADAMTS-1 to the nucleus, contrasting the pattern observed in the control cells.

Table 1 -

Cell lines

Cell Line	Organism	Cell type	Morphology	Tissue	Disease	Ref
HEK293T	*Homo sapiens*, human	Epithelial cells	Epithelial	Kidney	Normal tissue	ATCC CRL-11268
HTR-8	*Homo sapiens*, human	Trophoblast	Epithelial-like	Placenta	Normal tissue	ATCC CRL-3271
MCF7	*Homo sapiens*, human	Pleural effusion	Epithelial	Breast	Adenocarcinoma	ATCC HTB-22
MCF10	*Homo sapiens*, human	Epithelial cells	Epithelial	Breast	Normal tissue	ATCC CRL-10317
MDAH2774	*Homo sapiens*, human	Cells in the ascitic fluid	Epithelial	Ovary	Adenocarcinoma	Cellosaurus CVCL_0420
MDA-MB-231	*Homo sapiens*, human	Epithelial (EMT)	Epithelial	Breast	Adenocarcinoma	ATCC CRM-HTB-26
NIH-OVCAR-3	*Homo sapiens*, human	Epithelial cell	Epithelial	Ovary	Adenocarcinoma	ATCC HTB-161
Fibroblast	*Homo sapiens*, human	Fibroblast	Mesenchymal	Breast	Normal tissue	Ref. 23
HT1080	*Homo sapiens*, human	Fibroblast	Mesenchymal-like	Connective tissue	Fibrossarcoma	ATCC CCL-121
MuM-2B	*Homo sapiens*, human	Melanocytes	Mesenchymal-like	Ocular	Uveal melanoma	Cellosaurus CVCL_3447

ATCC (The American Type Culture Collection)

The Cellosaurus is part of the SIB Biodata Infrastructure and a SIB Resource

EMT: epithelial-to-mesenchymal transition